

A Comparison of Dry Snow Emission Model With Field Observations

Lingmei JIANG^{1,2}, J Shi², Saibun Tjuatja³, K.S Chen⁴

1. Research Center for Remote Sensing and GIS, School of Geography, Beijing Normal University, China

2. Institute for Computational Earth System Science, University of California, Santa Barbara, U.S.A

3. Department of Electrical Engineering, the University of Texas at Arlington, U.S.A

4. Center for Space and Remote Sensing Research, National Central University, Chung-Li, 32054

Abstract — In this paper, we evaluate the capability of the microwave emission model that including the Dense Media Radiative Transfer Model (DMRT) and AIEM for simulation of dry snow emissivity. We compared the model predictions with the ground experimental measurements. The comparison shows our snow microwave emission model agrees quite well with the measurements.

Keywords- snow; passive microwave remote sensing;

I. INTRODUCTION

Remote sensing retrieval of snow parameters, such as snow extent, snow water equivalent, and wet/dry state, has been investigated by many researchers using various microwave sensors with various degree of success [1-5]. Passive microwave remote sensing can provide useful information on snow cover characteristics for hydrological, climatological, and meteorological applications.

Microwave brightness temperature measurements between 3 GHz and 90 GHz have found sensitive to snow type and water equivalent [6]. At the lower frequencies of the microwave band, emission from a dry snow cover is mainly affected by underlying soil dielectric and roughness properties. At the higher frequencies, however, emission is sensitive to snow water equivalence and snow particle size since the volume scattering by snow particles becomes important [7], [8]. When snow starts to melt, emission will significantly increase due to the high dielectric contrast between ice and liquid water in microwave spectrum and the observed signals are only emitted from the near snow surface [9].

In order to simulate microwave emission signals reliably, it is necessary to validate the microwave models. In this study, we compared our microwave emission model with the ground measurements from the experiment [15].

II. MODEL DESCRIPTION

The snow emission model we used was based on Matrix Doubling Matrix method [10] which considers multi-scattering effects. In this model, we used the dense media model with the Mie scattering assumption [11] to describe snow pack extinction and emission properties for the vector radiative transfer model. The advanced Integral Equation Model (AIEM) [12] is used to calculate the subsurface emission

signal, and to calculate the boundary conditions at the snow-air and snow-soil interfaces for the model.

The snow layer was modeled as a closely packed irregular inhomogeneous layer above a homogeneous half space (see Figure 1). There were three major emission sources: upwelling and downwelling of emitted intensities within the snow layer; upward emission from the lower half space. These intensities were expected to go through some or all of the following processes, volume scattering, surface scattering, attenuation, surface-volume interactions and transmission across irregular boundary or boundaries, before they arrive at the receiver.

A. Radiative Transfer Model

The scattered intensity \hat{F} due to the layer is related to the incident intensity I by

$$I^s(\theta_s, \phi_s) = \frac{1}{4\pi} \int_{4\pi} S_{T1}(\theta_s, \theta; \phi_s - \phi) I(\theta, \phi) d\Omega \quad (1)$$

where $S_{T1}(\theta_s, \theta; \phi_s - \phi)$ is the total scattering phase matrix of the irregular layer.

The total emission u_t into the medium due to u_u , u_d and u_l may be written as

$$u_t = L_u u_u + L_d u_d + L_l u_l \quad (2)$$

where L 's are the multiple scattering operators.

u_u : the total upward emission from the layer.

u_d : the total downward emission from the layer.

u_l : the emission from the lower homogeneous half space.

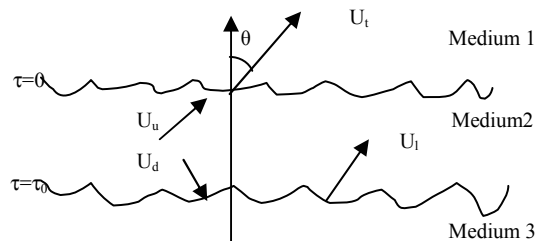


Fig.1 Geometry of the single layer emission problem.

The matrix-doubling method provides an alternative to the radiative transfer method for computing the combined scattering effects of surface and volume scattering. It is also

based on energy balance and has been shown to be an equivalent formulation to the radiative transfer approach [13]. In actual computation this is a more efficient method for layers having large optical thickness, but it is not suitable for extension to multilayered media.

B. The Advanced Integral Equation Model (AIEM)

At the interface between two homogeneous media, the scattering characteristics are determined by the interface roughness and the discontinuity between the media. Several surface scattering models have been developed in the last three decades [14]. They are the small perturbation model (SPM), Kirchhoff model (KM), phase perturbation model (PPM), full wave model (FWM), and the integral equation model (IEM) [10]. The IEM was verified by laboratory measurements of bistatic scattering from surfaces with small, intermediate and large scale roughness. This advanced IEM kept the absolute phase term in Greens function, meaning which has more accurate than the old IEM. So we applied AIEM to deal with boundary effects in this study.

The bistatic scattering coefficient can be expressed as

$$\sigma_{qp}^s = \sigma_{qp}^k + \sigma_{qp}^{kc} + \sigma_{qp}^c = \frac{k_1^2}{2} \exp\left[-\sigma^2(k_z^2 + k_{sz}^2)\right] \sum_{n=1}^{\infty} \sigma^{2n} \left| I_{qp}^n \right|^2 \frac{W^{(n)}(k_{sx} - k_x, k_{sy} - k_y)}{n!} \quad (3)$$

where

$$\begin{aligned} I_{qp}^n = & (k_{sz} + k_z)^n f_{qp} e^{-\sigma^2 k_z k_{sz}} \\ & + \frac{1}{4} \left\{ (k_{sz} - q_1)^n F_{qp1}^{(+)} e^{-\sigma^2 (q_1^2 - q_1 k_{sz} + q_1 k_z)} \right. \\ & + (k_{sz} - q_2)^n F_{qp2}^{(+)} e^{-\sigma^2 (q_2^2 - q_2 k_{sz} + q_2 k_z)} \\ & + (k_{sz} + q_1)^n F_{qp1}^{(-)} e^{-\sigma^2 (q_1^2 + q_1 k_{sz} - q_1 k_z)} \\ & + (k_{sz} + q_2)^n F_{qp2}^{(-)} e^{-\sigma^2 (q_2^2 + q_2 k_{sz} - q_2 k_z)} \\ & \left. + (k_{sz} + q_2)^n F_{qp2}^{(-)} e^{-\sigma^2 (q_2^2 + q_2 k_{sz} - q_2 k_z)} \right\} \Big|_{u,v=-k_x,-k_y} \\ & + \frac{1}{4} \left\{ (k_{sz} + q_1)^n F_{qp1}^{(+)} e^{-\sigma^2 (q_1^2 - q_1 k_{sz} + q_1 k_z)} \right. \\ & + (k_{sz} + q_2)^n F_{qp2}^{(+)} e^{-\sigma^2 (q_2^2 - q_2 k_{sz} + q_2 k_z)} \\ & + (k_{sz} - q_1)^n F_{qp1}^{(-)} e^{-\sigma^2 (q_1^2 + q_1 k_{sz} - q_1 k_z)} \\ & + (k_{sz} - q_2)^n F_{qp2}^{(-)} e^{-\sigma^2 (q_2^2 + q_2 k_{sz} - q_2 k_z)} \\ & \left. + (k_{sz} + q_2)^n F_{qp2}^{(-)} e^{-\sigma^2 (q_2^2 + q_2 k_{sz} - q_2 k_z)} \right\} \Big|_{u,v=-k_{sx},-k_{sy}} \quad (4) \end{aligned}$$

where $W^{(n)}(\bullet)$ is the Fourier transform of the n th power of the normalized surface correlation function. The above expression is suitable for small to large $k\sigma$ calculations. When $k\sigma$ is large, only the first term in eq. (4) can be kept in the formulation, which is the Kirchhoff term.

III. THE EXPERIMENTAL DATA DESCRIPTION

The radiometric measurements that we used for evaluation of our microwave model were from [15]. The ground data include temperature, permittivity, density and wetness profiles. The radiometric measurements were obtained with a set of five portable linearly polarized Dicke radiometers that operating at frequencies of 11, 21, 35, 48 and 94 GHz. The radiometers were fixed on a special sledge about 160 cm above ground. The incidence angle varies from 20° to 70°. These passive microwave measurements were complemented by ground observations and radar measurements. In this study, we used the measurements on Dec. 21, 1995 at Weissfluhjoch (46°49, 83°N, 9°48, 62°E) in Davos, Switzerland. These measurements were with four frequencies at both v- and h- polarizations, 11GHz, 21 GHz, 35GHz, 94 GHz.

IV. RESULT

A. Comparison with Ground Measurement Data.

TABLE I. SNOW PROFILE DATA FROM 21 DECEMBER 1995

Layer#	Tsnow(K)	W (%)	ρ (kg/m ³)	d(cm)
1	273.0	0.0	259.0	25.0
2	272.0	0.0	177.0	15.0
3	271.8	0.0	400.0	0.3
4	271.4	0.0	70.0	20.0

* T_{snow} is the snow temperature, W is the liquid water content, ρ the snow density, d the layer thickness. The layer number increases with height above ground

The snow profile data from [15] is shown in Table 1. It is a winter snow situation with a snow height of 60.3 cm. The top layer was 20 cm of new snow, below was a thin crust, and the bottom layer consisted of coarse-grained snow. Then we applied the following input parameters of the model:

- Density of snow: 0.22 g/cm³
- Radius: 0.48 mm
- Snow depth: 0.603m
- Snow temperature: 272.2 K
- Soil surface rms height and correlation length: 1, 20cm
- Soil moisture: 10%

The brightness temperature observed by radiometer (T_b) can be approximated described by the following expression:

$$T_b = T_s + (1-e) * T_{sky} \quad (5)$$

where T_s is the emission from snowpack and the underlying ground. T_{sky} is the downwelling atmospheric radiation. In this experiment, the sky brightness temperature is observed at 120° incidence angle for the used frequencies. The following are the comparison results.

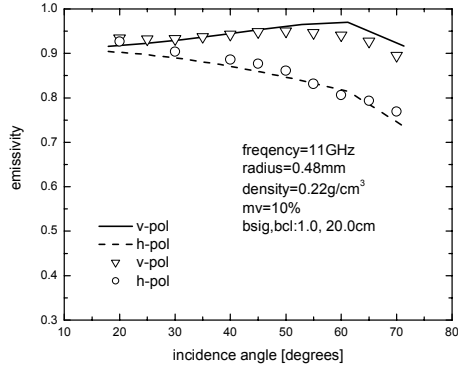


Fig2. Emissivity versus incidence angle at $f=11\text{GHz}$

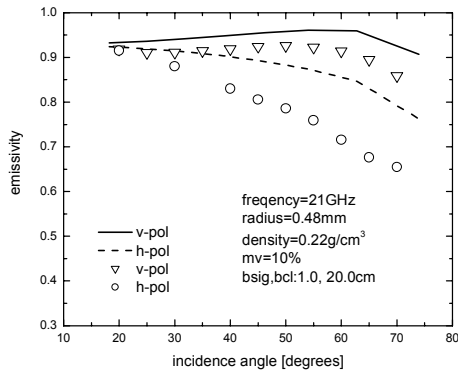


Fig3. Emissivity versus incidence angle at $f=21\text{GHz}$

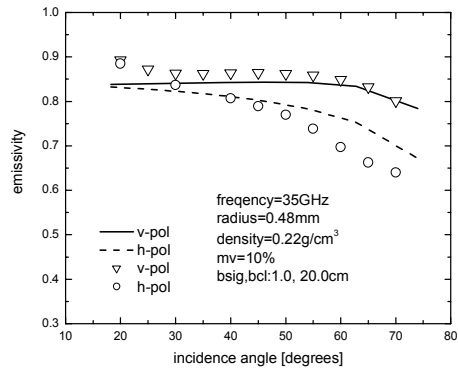


Fig4. Emissivity versus incidence angle at $f=35\text{GHz}$

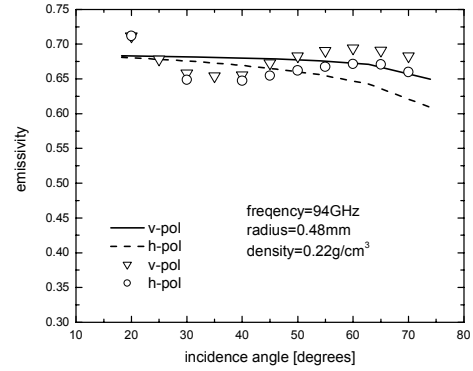


Fig5. Emissivity versus incidence angle at $f=94\text{GHz}$

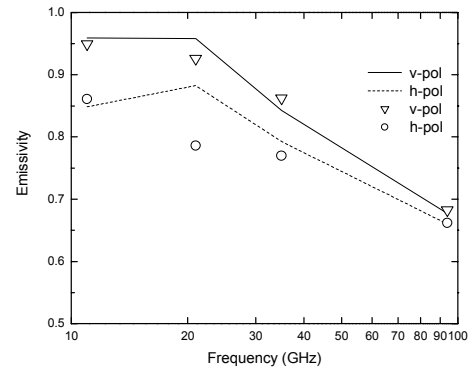


Fig6. Emissivity versus frequency at $\theta=50^\circ$.

Measured (circles and triangles) and simulated (curves) data of the snowpack of 21 December 1995

Figure 2, 3, 4 and 5 indicate the relationship of emissivity with incidence angle at 11 GHz, 21 GHz, 35 GHz and 94 GHz. Figure 6 is that emissivity varies with all the frequencies at 50° incidence angle. From these figures, we can see that:

From snow properties given in Table 1, we know the ground surface dielectric and roughness properties couldn't affect on the simulation at 94 GHz. It was found that the simulated emissivity at 94 GHz is very sensitive to snow density. Only a slight change in snow density will result in a significant change in the simulated emissivity. On the other hand, the ground surface dielectric and roughness properties have a great impact on the subsurface emission signals that may dominant at 11 GHz. At 11, 35, 94 GHz, our microwave emission model predictions agree well with the measured data in terms of both magnitudes for v and h-polarizations and their difference. It can be observed that as the frequency increases, the snow emissivity decreases and the difference between v and h polarizations also decreases. Or the emission signals between v and h polarizations become more closer as frequency increases.

At 21 GHz, the model simulated values are obviously higher than the measured data nearly for all incidence angles. It might result from the uncertainties in the experiment data at 21 GHz. The contribution from multiple scattering is expected to slow down the angular trend of horizontal emission but not vertical polarization [10]. From the measurements, the polarization difference with angular variation has the maximum at 21 GHz. The vertical emissivity at 21 GHz is higher than that at 11 GHz, while the horizontal emissivity is close to that at 35 GHz after 40° incidence angle. Such a result is not in agreement with intuition and our understanding. In addition, we can see the polarization difference at large incident angle decreased with the frequency increasing from 11 GHz to 94 GHz based on the model calculation value.

V. CONCLUSIONS

Experimental data on microwave emission from dry snow collected on Weissfluhjoch has been compared with theoretical simulations performed with our microwave emission model. The results indicate our model predicting dry snow emission signals fairly well.

ACKNOWLEDGMENTS

This work was supported by the project of the National Natural Science Foundation of China (90302008) and the Special Funds for Major State Basic Research Project (G2000077908).

REFERENCES

- [1] Goodison, B.E., A. Banga, and R.A. Halliday. 1984. Canada-United States Prairie Snow Cover Runoff Study. Canadian Water Resources Journal, Vol. 9, No. 1, pp. 99-107.
- [2] M. T. Hallikainen and P. Jolma, "Comparison of algorithms for retrieval of snow water equivalent from Nimbus-7 SMMR data in Finland," *IEEE Trans. Geosci. Remote Sensing*, vol. 30, pp.124-131, 1992.
- [3] A.T.C. Chang, J.L. Foster and D.K. Hall, "Nimbus-7 derived global snow cover parameters," *Annals of Glaciology*, vol. 9, pp. 39-44. 1987.
- [4] J. Aschbacher, "Land surface studies and atmospheric effects by satellite microwave radiometry," Ph. D. dissertation, Univ. of Innsbruck, 1989.
- [5] J.L. Foster, A.T.C. Chang and D.K. Hall, "Comparison of snow mass estimates from a prototype passive microwave snow algorithm, a revised algorithm and snow depth climatology," *Remote Sens. Environ.*, vol. 62, pp. 132-142, 1997.
- [6] G. Maceroni, S. Alasca, and et al, Microwave Emission From Dry Snow: A Comparison of Experimental and Model Results, *IEEE Trans. Geosci. Remote Sens.*, Vol. 39, No. 12, pp. 2649-2656, Dec., 2001.
- [7] R. Hofer and C. Matzler, "Investigation of snow parameters by radiometry in the 3- to 60-mm wavelength region," *J. Geophys. Res.*, vol. 85, pp. 453-460, 1980.
- [8] H. Rott and K. Sturm, "Microwave signature measurements of Antarctic and Alpine snow," in Proc. 11th EARSeL Symp., Graz, Austria, 1991, pp. 140-151.
- [9] M. T. Hallikainen, F. T. Ulaby, and T. E. Van Deventer, "Extinction behavior of dry snow in the 18-90 GHz range," *IEEE Trans Geosci. Remote Sensing*, vol, GE-25, pp.737-745, 1987.
- [10] A. K. Fung, *Microwave Scattering and Emission Models and Their Applications*. Norwood, MA: Artech House, 1994.
- [11] L. Tsang, "Dense media radiative transfer theory for dense discrete random media with particles of multiple sizes and permittivities," *Prog. Electromag. Res.* 6, vol. 5, pp. 181-225, 1992.
- [12] K. S. Chen, T. D. Wu, et al., "Emission of rough surfaces calculated by the Integral Equation Method with comparison to three-dimensional moment method simulations", *IEEE trans. Geosci. Remote Sens.*, vol. 41, no. 3, pp. 90-101, 2003.
- [13] Twomey, S., H. Jacobowitz and H. B. Howell, "Matrix Methods for Multiple-Scattering Problems", *J. Atmos. Sci.*, Vol. 23, pp.289-296, 1966.
- [14] Ulaby, F.T., R.K. Moore and A. k. Fung, *Microwave remote sensing*, vol.2, Artech House. Norwood, MA, 1982, Chapter 12.
- [15] Wiesmann, A., Stozzi, T., and Weise, T. (1996), *Passive microwave signature catalogue of snowcovers at 11, 21, 35, 48 and 94 Ghz*, IAP Research Report 96-8, University of Bern, Switzerland.